

## Profile measurement of aspheric surfaces using scanning deflectometry and rotating autocollimator with wide measuring range

This content has been downloaded from IOPscience. Please scroll down to see the full text.

2014 Meas. Sci. Technol. 25 064008

(<http://iopscience.iop.org/0957-0233/25/6/064008>)

View [the table of contents for this issue](#), or go to the [journal homepage](#) for more

Download details:

IP Address: 133.11.77.52

This content was downloaded on 04/07/2014 at 02:57

Please note that [terms and conditions apply](#).

# Profile measurement of aspheric surfaces using scanning deflectometry and rotating autocollimator with wide measuring range

Kyohei Ishikawa<sup>1</sup>, Tomohiko Takamura<sup>1</sup>, Muzheng Xiao<sup>2</sup>, Satoru Takahashi<sup>1</sup> and Kiyoshi Takamasu<sup>1</sup>

<sup>1</sup> Department of Precision Engineering, The University of Tokyo, Tokyo 113-8656, Japan

<sup>2</sup> School of Mechanical Engineering, Beijing Institute of Technology, Beijing 100081, People's Republic of China

E-mail: [ishikawa@nanolab.t.u-tokyo.ac.jp](mailto:ishikawa@nanolab.t.u-tokyo.ac.jp)

Received 29 October 2013, revised 17 February 2014

Accepted for publication 20 February 2014

Published 30 April 2014

## Abstract

High-accuracy aspherical mirrors and lenses with large dimensions are widely used in large telescopes and other industry fields. However, the measurement methods for large aspherical optical surfaces are not well established. Scanning deflectometry is used for measuring optical signals near flat surfaces with uncertainties on subnanometer scales. A critical issue regarding scanning deflectometry is that high-accuracy autocollimators (AC) have narrow angular measuring ranges and are not suitable for measuring surfaces with large slopes and angular changes. The goal of our study is to measure the profile of large aspherical optical surfaces with an accuracy of approximately 10 nm. We have proposed a new method to measure optical surfaces with large aspherical dimensions and large angular changes by using a scanning deflectometry method. A rotating AC was used to increase the allowable measuring range. Error analysis showed that the rotating AC reduces the accuracy of the measurements. In this study, we developed a new AC with complementary metal-oxide semiconductor (CMOS) as a light-receiving element (CMOS-type AC). The CMOS-type AC can measure wider ranges of angular changes, with a maximum range of 21 500  $\mu\text{rad}$  (4500 arcsec) and a stability (standard deviation) of 0.1  $\mu\text{rad}$  (0.02 arcsec). We conducted an experiment to verify the effectivity of the wide measuring range AC by the measurement of a spherical mirror with a curvature radius of 500 mm. Furthermore, we conducted an experiment to measure an aspherical optical surface (an off-axis parabolic mirror) and found an angular change of 0.07 rad (4 arcdegrees). The repeatability (average standard deviation) for ten measurements of the off-axis parabolic mirror was less than 4 nm.

Keywords: large aspherical surface, profile measurement, scanning deflectometry, autocollimator

(Some figures may appear in colour only in the online journal)

## Nomenclature

		$D$	Distance between rotation center of rotary stage and surface under measurement.
CMOS	Complementary metal-oxide semiconductor.	$R$	Curvature radius.
$\alpha$	Angle of rotation by rotary stage.	$k$	Slope of least square line.
$S$	Distance of moved measurement point by rotation of autocollimator.	$\beta$	Angular change of autocollimator on rotation part.
$A$	Angular change caused by the distance change by rotation of autocollimator.	$\theta$	Angular change from curvature center.
		$f$	Curve profile.
		$\sigma$	Profile error.

$E_a$	Stability of autocollimator.
$E_A$	Angle error.
$E_R$	Rotating angle error.
$E_x$	Positioning error of linear stage.
$E_p$	Pitching error of linear stage.
$E_c$	Connected angle error.
$N$	Number of sampling points.
$h$	Scanning interval.
$L$	Scanning length.

### 1. Introduction

Large, high-precision aspherical mirrors and lenses, such as the mirrors for reflecting telescopes and the lenses for semiconductor exposure apparatuses, are used in advanced technology industries. Nowadays, the required accuracy of these surfaces is on the order of tens of nanometers. However, the measurement methods for these surfaces are not well established. Scanning deflectometry is used for measuring optical properties on or near flat surfaces with uncertainties on subnanometer scales [1–6]. A critical issue in scanning deflectometry is that high-accuracy autocollimators (AC) have narrow angular measuring ranges and are therefore not suitable for measuring surfaces with large slopes and angular changes [7–11].

The measurement targets of our study are aspherical optical surfaces with diameters greater than 300 mm and angular changes greater than 200 mrad. The desired measurement uncertainty in the vertical direction is less than 10 nm. In this paper, we propose a measurement method based on scanning deflectometry to increase the measurement range of the AC. First, we introduce the principles of the proposed method as well as a data processing method.

Then, we discuss a newly developed AC with CMOS as an optical image element (CMOS-type AC). The CMOS-type AC can measure wide angular ranges, with a maximum measuring range of 21 500  $\mu\text{rad}$  (4500 arcsec) and a stability (standard deviation) of 0.1  $\mu\text{rad}$  (0.02 arcsec). We conducted experiments to evaluate the effectiveness of the wide measuring range AC by the measurement of a spherical mirror with a curvature radius of 500 mm. Furthermore, we conducted an experiment to measure an aspherical optical surface (an off-axis parabolic mirror) with an angular change of 0.07 rad (4 arcdegrees), by using the CMOS-type AC. The repeatability for ten measurements of an off-axis parabolic mirror was less than 4 nm.

### 2. Principle

#### 2.1. Measurement principles

The basic measurement principle is shown in figure 1 [12, 13]. A rotary stage is fixed on a linear stage. On the rotary stage, an AC is fixed, and by translation of the linear stage, the surface is measured. When measuring surfaces with large slopes, the rotary stage is used to help increase the measuring range. When the angle measured with the AC exceeds the maximum range, the rotary stage turns a certain angle. Consequently, the

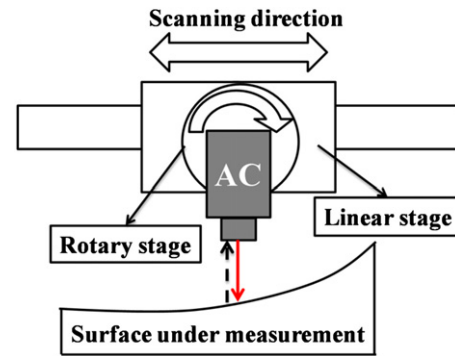


Figure 1. Principle of the rotary AC method for increasing measuring range of the deflectometry method.

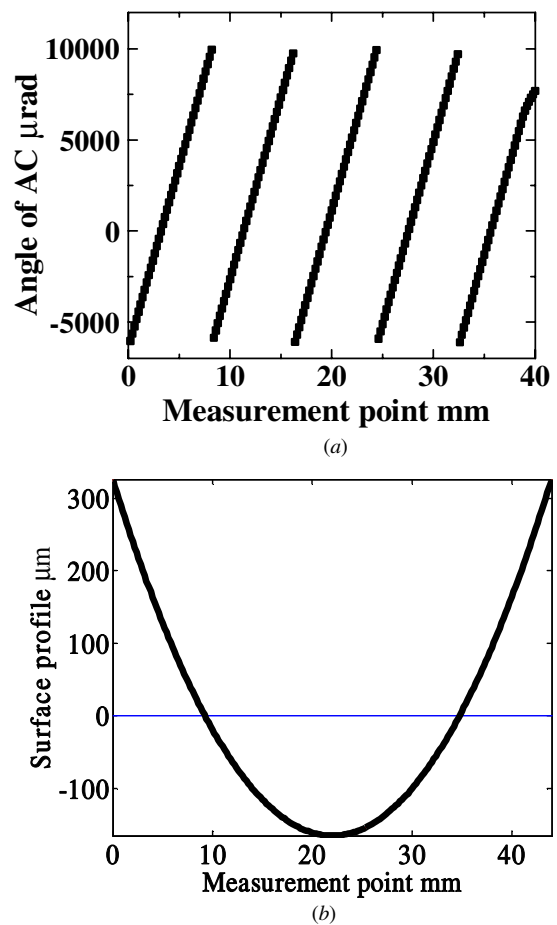


Figure 2. Profile measurement by rotating AC. (a) Angle data measured by autocollimator. (b) Profile data with subtracted least square line.

measured angle returns into the allowable measuring range. Then, by linear translation, scanning of the whole surface continues. Integrating the angle data gives the profile of the optical surface.

Figure 2(a) shows the angular data measured from the AC. Because the AC rotates, the measured angle is not continuous. The connected angle data are calculated from the measured angle. Then the profile data in figure 2(b) are calculated by integrating the connected angle data.

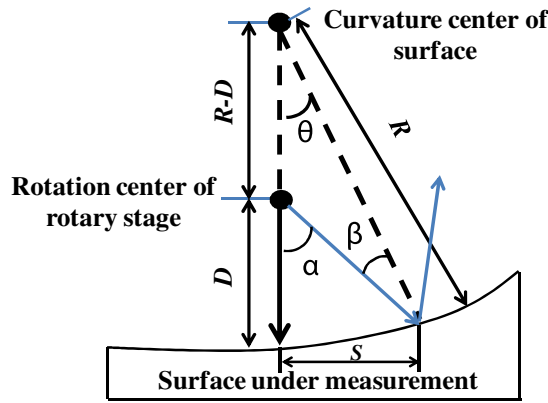


Figure 3. Relationships between angles  $\alpha$  and  $\beta$  when the AC rotation angle is  $\theta$ .

2.2. Connected angle [12]

The connection method used for the angle data is a key procedure of the proposed measurement method. Because the AC rotates, a ray of light turns a certain angle  $\alpha$ , so that the measured point also moves by  $S$ , as shown in figure 3. Consequently, the angle measured by the AC is interrupted by rotation. To connect the angular data, the distance moved  $S$ , caused by rotation, and the angular change  $A$ , caused by the change in distance must be known.

The repeatability of a motorized rotary stage with a wide range is usually large. Therefore, we have proposed a method to calculate the rotated angle  $\alpha$  of the rotary stage from the AC data. Because  $\theta$  is an angle on the order of several tens of thousands of microradians, we can assume that the circular arc length  $R\theta$  is the same as the circular arc length,  $\alpha D$ . Thus, the relationship between  $\alpha$  and  $\beta$  is given by

$$\alpha = \theta + \beta, \quad R\theta = \alpha D, \quad \alpha = \frac{R}{R-D}\beta \quad (1)$$

Here,  $\beta$  is read from the angle data and  $R$  is the reciprocal of the curvature. We calculated the displacement  $S$  and the according angular change  $A$ , using the following equations:

$$S = \alpha D = \frac{\beta D}{1 - kD} \quad (2)$$

$$A = kS = \frac{k\beta D}{1 - kD}. \quad (3)$$

3. Error analysis and simulation of measuring error

3.1. Propagation from the angle error to profile error [14]

We performed an error analysis to check what factors were sensitive to the measurement results. This was necessary before setting up the experimental device. The final surface profile error  $\sigma$  was a result of the connected angle error  $E_c$ .  $E_c$  was partly caused by the rotating angle error  $E_R$ . The angle error  $E_A$  also contributed to  $E_c$ . The AC error  $E_a$ , the positioning error of the linear stage  $E_x$  and the pitching error of the linear stage  $E_p$ , together determined the angle error  $E_A$ , as shown in the following equation:

$$E_A = \sqrt{E_a^2 + \left(\frac{E_x}{R}\right)^2 + E_p^2}. \quad (4)$$

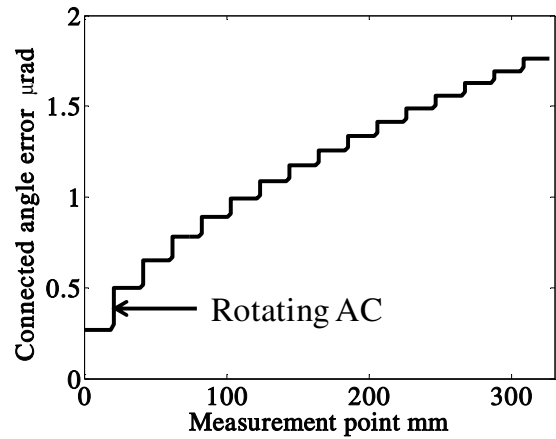


Figure 4. Angular error data from error analysis.

Table 1. Parameters for simulation of the surface profile error.

Parameter	Value
Scanning length $L$	300 mm
Curvature radius $R$	1000 mm
Scanning interval $h$	0.2 mm
Stability of autocollimator $E_a$	0.15 $\mu\text{rad}$
Positioning error of linear stage $E_x$	0.1 $\mu\text{m}$
Pitching error of linear stage $E_p$	0.2 $\mu\text{rad}$

If the radius of the measuring point is  $R$  and the positioning error of linear stage is  $E_x$ , the angle measured will differ by  $E_x/R$ . The profile data were calculated by numerically integrating the angle data. Simultaneously, the angle error  $E_a$  is propagated to the final surface profile error  $\sigma$ , as shown in the following equation [15],

$$\sigma = \sqrt{N}hE_c = \sqrt{h}LE_c, \quad (5)$$

where  $h$  is the sampling interval,  $N$  is the number of sampling points and  $L$  is the scanning length of the sample.

3.2. Simulation of the measuring error

An example is shown for the profile measurement error for a spherical surface 300 mm in length and a curvature radius of 1000 mm. We set the parameters as listed in table 1, according to the ordinary experimental devices. Figure 4 shows the connected angle error  $E_c$ .  $E_c$  increased with increased rotation of the AC. Figure 5 shows the final profile error. The calculated uncertainty (average standard deviation) in the profile measurement is 25 nm.

4. Development of CMOS-type AC

Error analysis showed that the angular error increased with increasing rotation of the AC. Therefore, we have developed a new AC with CMOS as an optical image element (CMOS-type AC). Figure 6 illustrates the conceptual design and the photograph of the CMOS-type AC. Table 2 lists specifications and table 3 lists performances of the CMOS-type AC. The structural design is simple and low-cost elements are selected. In addition, the CMOS image sensor is directly connected to

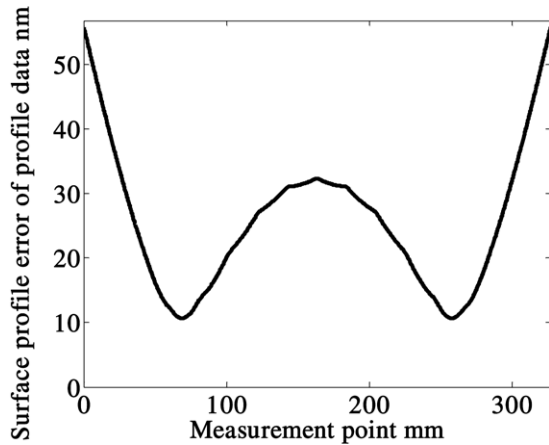


Figure 5. Surface profile error from error analysis.

Table 2. Specifications of the CMOS-type AC.

Specifications	Value
Size	40 (H) × 110 (W) × 150 (D) mm
Light source	LD (634 nm)
Diameter of beam	1.7 mm
Image element	CMOS (EO-5012), 2560 (H) × 1920 (V)
Focal length	100 mm

Table 3. Performance of CMOS-type AC.

Performance	Value
Measurement range	21 500 μrad
Stability	0.1 μrad
Pixel resolution	11.0 μrad
Calculated resolution	0.05 μrad

Table 4. Experimental conditions for effects by the rotation of AC.

Parameter	Value
Measurement target	Concave spherical mirror
Curvature radius <i>R</i>	500 mm
Scanning interval <i>h</i>	0.2 mm
Scanning length <i>L</i>	40 mm
Number of rotations of AC	4, 6, 8, 14

the personal computer by the USB interface. Therefore, the data processing system is simple and low cost.

Figure 7(a) shows the light image on the CMOS, and figure 7(b) shows the image signal distribution. The angle was calculated using the barycenter of the image spot. The calculated resolution was approximately 0.05 μrad, and the maximum measurement range was 21 500 μrad. Figure 8 shows the stability of the CMOS-type AC for a measurement made on a flat mirror. The mirror was measured in 1 h, and the standard deviation of the angle was 0.1 μrad.

## 5. Experiment

### 5.1. Experiment setup

An experimental setup was constructed, as shown in figure 9. The surface under measurement is fixed vertically in the

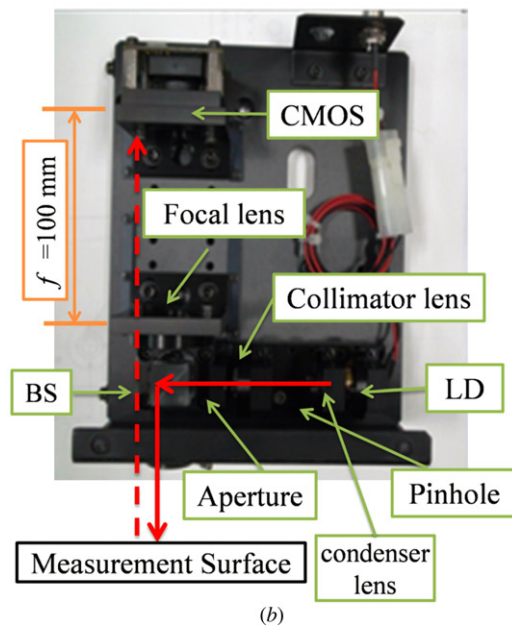
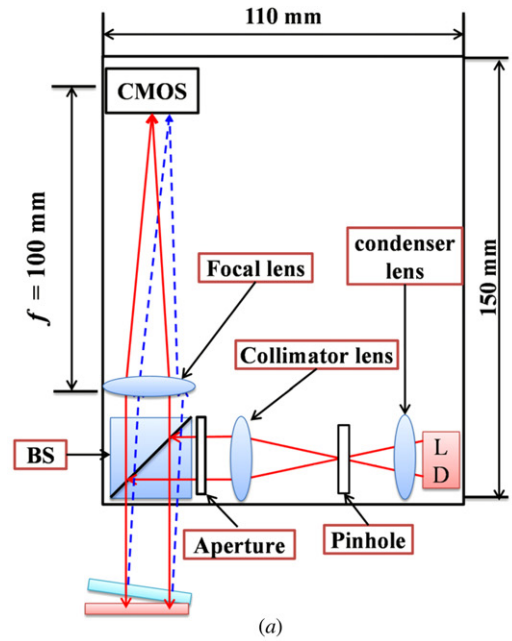


Figure 6. (a) Structural design and (b) photograph of developed CMOS-type AC.

holder. The linear stage is parallel to the base of the mirror. A motorized rotary stage with the CMOS-type AC is fixed on the linear stage. The laser coming from the CMOS-type AC is reflected by the surface under measurement, and the laser subsequently returns to the CMOS-type AC.

### 5.2. Effects of the rotation of AC

The number of rotations of AC affects the accuracy of profile measurements. The effect of the rotation of AC is evaluated by limitation of the measurement range of AC. Table 4 lists the experimental conditions for the evaluation. A concave spherical mirror with a radius of 500 mm was measured in a scanning distance of 40 mm. When the full measuring range (21 500 μrad) of AC is used, the number of rotations is four

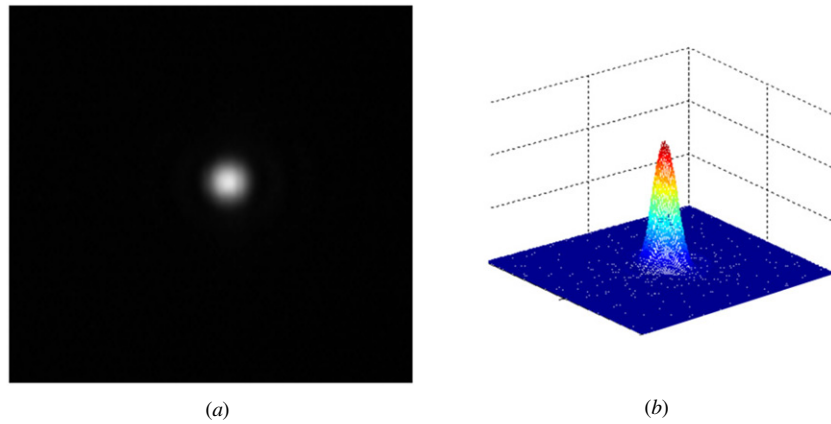


Figure 7. Beam image on CMOS. (a) Image spot on CMOS. (b) Image signal distribution.

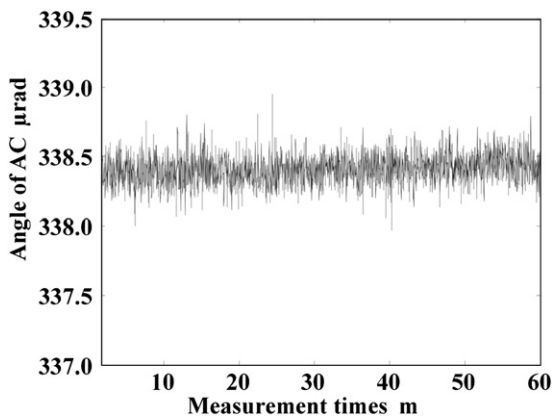


Figure 8. Stability of CMOS-type AC over 1 h is 0.1  $\mu\text{rad}$ .

times. The measuring range is limited by 20 000, 16 000, 10 000 and 8000  $\mu\text{rad}$ . Therefore, the numbers of rotations are 4, 6, 8 and 14, respectively. Table 5 shows the standard deviation of the profile over ten measurements with the number of rotations of AC. The relationship between the repeatability of profile measurements and the number of rotations is evaluated by the experiments. Then the effectiveness of wide measuring range AC is verified.

Table 5. Repeatability for the number of rotations of AC.

Limitation of measuring range of AC ( $\mu\text{rad}$ )	Number of rotations	Standard deviation of profile data (10 times) (nm)
20 000	4	1.93
16 000	6	2.07
10 000	8	2.54
8000	14	5.15

To verify the error analysis, we compared the estimated error and experimental error. We assumed that the stability (standard deviation) of the AC  $E_a$  was 0.15  $\mu\text{rad}$ , the positioning error of the linear stage  $E_x$  was 0.1  $\mu\text{m}$  and the pitching error of the linear stage  $E_p$  was 0.2  $\mu\text{rad}$  for the error analysis. Figure 10 shows the standard deviation for ten measurements in the experiment and the surface profile error in the error analysis. In both sets of data, agreement in the profile of the graph and the values is shown. The feasibility of the error analysis was confirmed by this comparison.

### 5.3. Profile measurement of off-axis parabolic mirror

An off-axis parabolic mirror with a diameter of 50.8 mm was measured. The profile of the mirror is illustrated in figure 11.

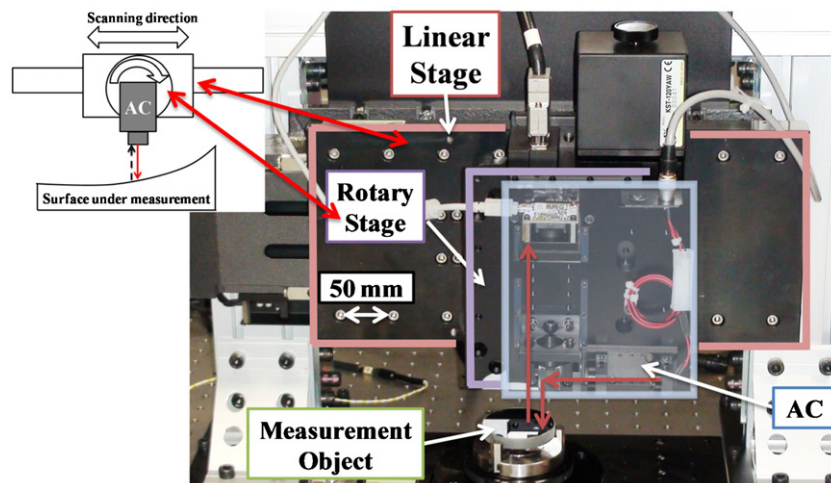


Figure 9. Experimental setup with CMOS-type A.

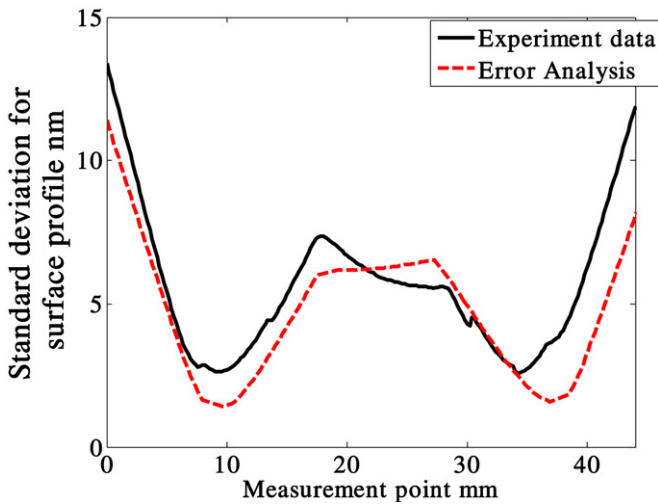


Figure 10. Standard deviation for ten measurements of surface profile of mirror with radius of 500 mm, along with error analysis.

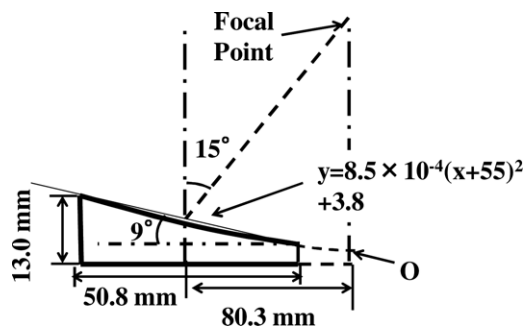


Figure 11. Profile of measurement object (off-axis parabolic mirror).

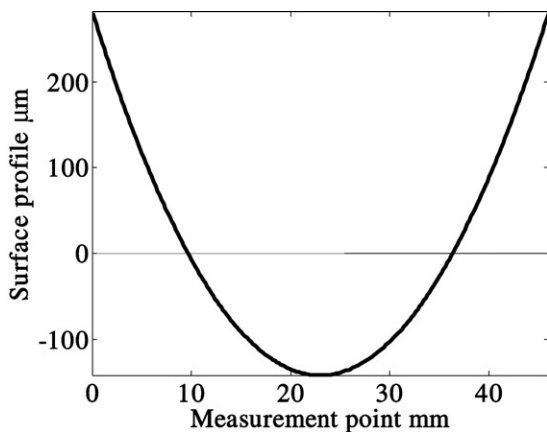


Figure 12. Measured profile of off-axis parabolic mirror.

Table 6. Experimental conditions for the off-axis parabolic mirror

Parameter	Value
Measurement target	Off-axis parabolic mirror
Angular change	0.07 rad
Scanning interval $h$	0.2 mm
Scanning length $L$	40 mm
Number of rotations of AC	4

The angular change was approximately 0.07 rad, the scanning length  $L$  was 40 mm and the scanning step  $h$  was 0.2 mm (see

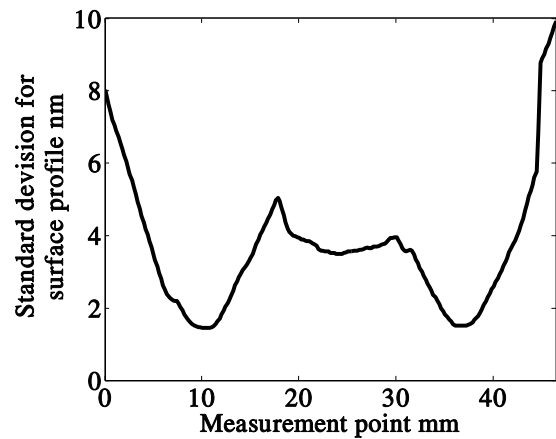


Figure 13. Standard deviation for ten measurements of the surface profile of the off-axis parabolic mirror.

table 6). Figure 12 shows the measured surface profile, and figure 13 shows the standard deviation of ten measurements. The repeatability (average standard deviation) of the profile was less than 4.0 nm.

## 6. Conclusion

We proposed a new method of measuring large aspherical optical surfaces using a rotating AC; the method is based on a scanning deflectometry method. Error analysis was performed to estimate the measurement uncertainty. To reduce the error of the profile, we developed a CMOS-type AC system with a wide measuring range. The measuring range of the developed CMOS-type AC is 21 500  $\mu$ rad. We conducted experiments to evaluate the effectiveness of the wide measuring range AC by the measurement of a spherical mirror with a curvature radius of 500 mm. From the comparison between the error analysis and the measured results for the spherical mirror, we confirmed the feasibility of the error analysis and the viability of nanometer profile measurements using the proposed method. Furthermore, we measured the surface profile of an off-axis parabolic mirror having an angular change of 0.07 rad. The repeatability (average standard deviation) was less than 4.0 nm.

## References

- [1] Geckeler R 2006 ESAD shearing deflectometry: potentials for synchrotron beamline metrology *Proc. SPIE* **6317** 6317H
- [2] Geckeler R D, Just A, Krause M and Yashchuk V V 2010 Autocollimators for deflectometry: current status and future progress *Nucl. Instrum. Methods Phys. Res. A* **616** 140–6
- [3] Siewert F, Buchheim J, Höft T, Fiedler D, Bourenkov G, Cianci M and Signorato R 2012 High angular resolution slope measuring deflectometry for the characterization of ultra-precise reflective x-ray optics *Meas. Sci. Technol.* **23** 074015
- [4] Ehret G, Schulz M, Stavridis M and Elster C 2012 Deflectometric systems for absolute flatness measurements at PTB *Meas. Sci. Technol.* **23** 094007
- [5] Schulz M, Ehret G and Fitzenreiter A 2010 Scanning deflectometric form measurement avoiding path-dependent angle measurement errors *J. Eur. Opt. Soc. Rapid Publ.* **5** 10026

- [6] Polack F, Thomasset M, Brochet S and Rommeveaux A 2010 An LTP stitching procedure with compensation of instrument errors: comparison of SOLEIL and ESRF results on strongly curved mirrors *Nucl. Instrum. Methods Phys. Res. A* **616** 207–11
- [7] Trakas P Z, Curch E L, Bresloff C J and Assoufid L 1999 Improvements in the accuracy and the repeatability of long trace profiler measurements *Appl. Opt.* **38** 5468
- [8] Siewert F, Buchheim J, Zeschke T, Brenner G, Kapitzki S and Tiedtke K 2011 Sub-nm accuracy metrology for ultra-precise reflective x-ray optics *Nucl. Instrum. Methods Phys. Res. A* **635** S52–7
- [9] Siewert F, Buchheim J, Boutet S, Williams M G J, Montanez P, Krzywinski J and Signorato R 2012 Ultra-precise characterization of LCLS hard x-ray focusing mirrors by high resolution slope measuring deflectometry *Opt. Express* **20** 4525
- [10] Siewert F, Buchheim J, Hoft T, Fiedler S, Bourenkov G, Cianciand M and Signorato R 2012 High angular resolution slope measuring deflectometry for the characterization of ultra-precise reflective x-ray optics *Meas. Sci. Technol.* **23** 074015
- [11] Gao W, Huang P S, Yamada T and Kiyono S 2002 A compact and sensitive two-dimensional angle probe for flatness measurement of large silicon wafers *Precis. Eng.* **26** 396–404
- [12] Xiao M, Jujo S, Takahashi S and Takamasu K 2012 Nanometer profile measurement of large aspheric optical surface by scanning deflectometry with rotatable devices: uncertainty propagation analysis and experiments *Precis. Eng.* **36** 91–6
- [13] Xiao M, Jujo S, Takamasu K and Takahashi S 2011 Nanometer profile measurement of large aspheric optical surface by scanning deflectometry with rotatable devices—error analysis and experiments *Proc. Euspen (Como, Italy)* pp 129–32
- [14] Xiao M, Takamura T, Takahashi S and Takamasu K 2013 Random error analysis of profile measurement of large aspheric optical surface using scanning deflectometry with rotary stage *Precis. Eng.* **37** 599–605
- [15] Ennos A E and Virdee M S 1986 Precision measurement of surface form by laser profilometry *Wear* **109** 275–86